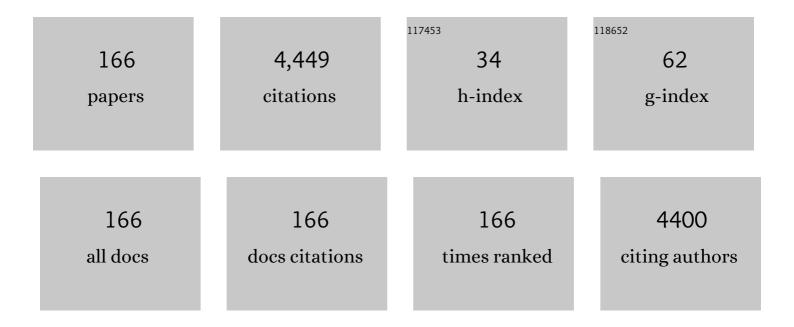
List of Publications by Year in descending order

Source: https://exaly.com/author-pdf/3442812/publications.pdf Version: 2024-02-01



#	Article	lF	CITATIONS
1	Systematic Investigation of Growth and Properties of Ga <sub>2</sub> O <sub>3</sub> Films on C-Plane Sapphire Substrates Prepared by Plasma-Assisted Molecular Beam Epitaxy. ECS Journal of Solid State Science and Technology, 2022, 11, 035008.	0.9	2
2	Highly Asymmetric Optical Properties of β-Ga <sub>2</sub> O <sub>3</sub> as Probed by Linear and Nonlinear Optical Excitation Spectroscopy. Journal of Physical Chemistry C, 2021, 125, 1432-1440.	1.5	16
3	Reduction of dislocations in α-Ga <sub>2</sub> O <sub>3</sub> epilayers grown by halide vapor-phase epitaxy on a conical frustum-patterned sapphire substrate. IUCrJ, 2021, 8, 462-467.	1.0	9
4	Strengthening and fracture of deformation-processed dual fcc-phase CoCrFeCuNi and CoCrFeCu1.71Ni high entropy alloys. Materials Science & Engineering A: Structural Materials: Properties, Microstructure and Processing, 2020, 781, 139241.	2.6	28
5	xmlns:mml="http://www.w3.org/1998/Math/MathML" altimg="si1.svg"> <mml:mrow><mml:mo stretchy="true"&gt;(<mml:mrow><mml:mover) 0.784314="" 1="" 10="" 50="" 582="" etqq1="" overlock="" rgbt="" td="" td<="" tf="" tj=""><td>(accent="tr</td><td>ue"&gt;<mml:m< td=""></mml:m<></td></mml:mover)></mml:mrow></mml:mo </mml:mrow>	(accent="tr	ue"> <mml:m< td=""></mml:m<>
6	Nanoscale modulated structures by balanced distribution of atoms and mechanical/structural stabilities in CoCuFeMnNi high entropy alloys. Materials Science & amp; Engineering A: Structural Materials: Properties, Microstructure and Processing, 2019, 762, 138120.	2.6	34
7	Effect of in situ annealing on the structural properties of Bi2Te3 films grown on (0â€ <sup>-</sup> 0â€ <sup>-</sup> 0â€ <sup>-</sup> 1) sapphire. Journal of Crystal Growth, 2019, 525, 125191.	0.7	1
8	Effects of nanoepitaxial lateral overgrowth on growth of <b> <i>α</i> </b> -Ga2O3 by halide vapor phase epitaxy. Applied Physics Letters, 2019, 115, .	1.5	17
9	Precipitation and decomposition in CoCrFeMnNi high entropy alloy at intermediate temperatures under creep conditions. Materialia, 2019, 8, 100445.	1.3	22
10	Growth and characterization of gallium oxide films grown with nitrogen by plasma-assisted molecular-beam epitaxy. Thin Solid Films, 2019, 682, 93-98.	0.8	19
11	Growth of single crystal non-polar ( <mmi:math )="" eiqq<="" ij="" td="" xmins:mml="http://www.w3.org/1998/Math/MathML"><td>3.1</td><td>10 10</td></mmi:math>	3.1	10 10
12	Effects of Growth Rate and III/V Ratio on Properties of AlN Films Grown on c-Plane Sapphire Substrates by Plasma-Assisted Molecular Beam Epitaxy. Korean Journal of Materials Research, 2019, 29, 579-585.	0.1	1
13	Epitaxial Growth of Bandgap Tunable ZnSnN <sub>2</sub> Films on (0001) Al <sub>2</sub> O <sub>3</sub> Substrates by Using a ZnO Buffer. Crystal Growth and Design, 2018, 18, 1385-1393.	1.4	18
14	Microstructural Investigation of CoCrFeMnNi High Entropy Alloy Oxynitride Films Prepared by Sputtering Using an Air Gas. Metals and Materials International, 2018, 24, 1285-1292.	1.8	13
15	Structural Characterization of CoCrFeMnNi High Entropy Alloy Oxynitride Thin Film Grown by Sputtering. Korean Journal of Materials Research, 2018, 28, 595-600.	0.1	1
16	In Situ Oxidation of GaN Layer and Its Effect on Structural Properties of Ga2O3 Films Grown by Plasma-Assisted Molecular Beam Epitaxy. Journal of Electronic Materials, 2017, 46, 3499-3506.	1.0	5
17	Depth dependent strain analysis in GaN-based light emitting diodes using surface-plasmon enhanced Raman spectroscopy. Physica Status Solidi (A) Applications and Materials Science, 2017, 214, 1600805.	0.8	4
18	Simultaneous determination of defect distributions and energies near InGaN/GaN quantum wells by capacitance–voltage measurement. Journal Physics D: Applied Physics, 2017, 50, 39LT03.	1.3	1

#	Article	IF	CITATIONS
19	Thermally activated deformation and the rate controlling mechanism in CoCrFeMnNi high entropy alloy. Materials Science & Engineering A: Structural Materials: Properties, Microstructure and Processing, 2017, 682, 569-576.	2.6	96
20	High Temperature Behavior of Injection and Radiative Efficiencies and Its Effects on the Efficiency Droop in InGaN/GaN Light Emitting Diodes. Journal of Nanoscience and Nanotechnology, 2016, 16, 11640-11644.	0.9	2
21	A Hydrogen Sulfide Gas Sensor Based on Pd-Decorated ZnO Nanorods. Journal of Nanoscience and Nanotechnology, 2016, 16, 10351-10355.	0.9	17
22	Effects of growth pressure on morphology of ZnO nanostructures by chemical vapor transport. Chemical Physics Letters, 2016, 658, 182-187.	1.2	12
23	Strain mapping in a nanoscale-triangular SiGe pattern by dark-field electron holography with medium magnification mode. Microscopy (Oxford, England), 2016, 65, 499-507.	0.7	2
24	Three-Dimensional Hierarchical Structures of TiO <sub>2</sub> /CdS Branched Core-Shell Nanorods as a High-Performance Photoelectrochemical Cell Electrode for Hydrogen Production. Journal of the Electrochemical Society, 2016, 163, H434-H439.	1.3	20
25	Co3O4–SWCNT composites for H2S gas sensor application. Sensors and Actuators B: Chemical, 2016, 222, 166-172.	4.0	75
26	Comprehensive Study of the Surface Morphology Evolution Induced by Thermal Annealing in <i>A</i> -Plane ZnO Films on <i>R</i> -Plane Al <sub>2</sub> O <sub>3</sub> Substrates. Science of Advanced Materials, 2016, 8, 358-362.	0.1	2
27	Characterization of Basal Plane Dislocations in PVT-Grown SiC by Transmission Electron Microscopy. Korean Journal of Materials Research, 2016, 26, 656-661.	0.1	0
28	Fabrication and Photoelectrochemical Properties of a Cu2O/CuO Heterojunction Photoelectrode for Hydrogen Production from Solar Water Splitting. Korean Journal of Materials Research, 2016, 26, 604-610.	0.1	3
29	2D strain measurement in sub-10Ânm SiGe layer with dark-field electron holography. Current Applied Physics, 2015, 15, 1529-1533.	1.1	1
30	Effect of indium concentration on morphology of ZnO nanostructures grown by using CVD method and their application for H2 gas sensing. Superlattices and Microstructures, 2015, 82, 349-356.	1.4	13
31	Photoelectrochemical water splitting properties of hydrothermally-grown ZnO nanorods with controlled diameters. Electronic Materials Letters, 2015, 11, 65-72.	1.0	26
32	Investigation of the photoelectrochemical properties for typical ZnO nanostructures grown by using chemical vapor transport. Journal of the Korean Physical Society, 2015, 66, 832-838.	0.3	3
33	Growth and characterization of Mg Zn1â^'O films grown on r-plane sapphire substrates by plasma-assisted molecular beam epitaxy. Journal of Alloys and Compounds, 2015, 623, 1-6.	2.8	4
34	Comprehensive Structural Characterization of Commercial Blue Light Emitting Diode by Using High-Angle Annular Dark Filed Scanning Transmission Electron Microscopy and Transmission Electron Microscopy. Korean Journal of Materials Research, 2015, 25, 1-8.	0.1	0
35	Crystal orientation variation of nonpolar AlN films with III/V ratio on r-plane sapphire substrates by plasma-assisted molecular beam epitaxy. Electronic Materials Letters, 2014, 10, 1109-1114.	1.0	4
36	Experimental verification of effects of barrier dopings on the internal electric fields and the band structure in InGaN/GaN light emitting diodes. Applied Physics Letters, 2014, 104, .	1.5	8

#	Article	IF	CITATIONS
37	Effect of First-Stage Growth Manipulation and Polarity of SiC Substrates on AlN Epilayers Grown Using Plasma-Assisted Molecular Beam Epitaxy. Korean Journal of Materials Research, 2014, 24, 266~270-266~270.	0.1	1
38	Growth and stuctural characterization of InGaN layers with controlled In content prepared by plasma-assisted molecular beam epitaxy. Thin Solid Films, 2013, 546, 42-47.	0.8	2
39	Microstructural Characterization of High Indium-Composition InXGa1â^'XN Epilayers Grown on c-Plane Sapphire Substrates. Microscopy and Microanalysis, 2013, 19, 145-148.	0.2	4
40	Surface Polarity Effects on the Hydride Vapor Phase Epitaxial Growth of GaN on 6H-SiC with a Chrome Nitride Buffer Layer. Electrochemical and Solid-State Letters, 2012, 15, H148.	2.2	2
41	Hydrothermal Synthesis of ZnO Nanorods in the Presence of a Surfactant. Journal of Nanoscience and Nanotechnology, 2012, 12, 1328-1331.	0.9	2
42	Well-to-well non-uniformity in InGaN/GaN multiple quantum wells characterized by capacitance-voltage measurement with additional laser illumination. Applied Physics Letters, 2012, 100,	1.5	31
43	Tin Oxide-Carbon Nanotube Composite for NO <sub><i>X</i></sub> Sensing. Journal of Nanoscience and Nanotechnology, 2012, 12, 1425-1428.	0.9	26
44	Lattice Deformation in \$a\$-Plane ZnO Films Grown on \$r\$-Plane Al\$_{2}\$O\$_{3}\$ Substrates Grown by Plasma-Assisted Molecular-Beam Epitaxy. Applied Physics Express, 2012, 5, 081101.	1.1	6
45	Comprehensive Study about the Effect of Heat Treatment on the Electrical Properties of Single-Crystalline ZnO Materials. Applied Physics Express, 2012, 5, 075801.	1.1	3
46	Realization of an open space ensemble for nanowires: a strategy for the maximum response in resistive sensors. Journal of Materials Chemistry, 2012, 22, 6716.	6.7	60
47	Comprehensive study of the surface morphology evolution induced by thermal annealing in single-crystalline ZnO Films and ZnO bulks. Journal of the Korean Physical Society, 2012, 61, 1732-1736.	0.3	4
48	Improvement of Light Extraction Efficiency and Reduction of Leakage Current in GaN-Based LED Via V-Pit Formation. IEEE Photonics Technology Letters, 2012, 24, 449-451.	1.3	25
49	Optimization of a zinc oxide urchin-like structure for high-performance gas sensing. Journal of Materials Chemistry, 2012, 22, 1127-1134.	6.7	73
50	Selected Peer-Reviewed Articles from the International Union of Materials Research Societies—International Conference on Electronic Materials 2010 (IUMRS-ICEM 2010). Journal of Nanoscience and Nanotechnology, 2012, 12, 1128-1130.	0.9	0
51	Transparent Nanoscale Floating Gate Memory Using Selfâ€Assembled Bismuth Nanocrystals in Bi <sub>2</sub> Mg <sub>2/3</sub> Nb <sub>4/3</sub> O <sub>7</sub> (BMN) Pyrochlore Thin Films Grown at Room Temperature. Advanced Materials, 2012, 24, 3396-3400.	11.1	5
52	Heteroepitaxial growth of GaN on various powder compounds (AlN, LaN, TiN, NbN, ZrN, ZrB 2 , VN, BeO) by hydride vapor phase epitaxy. Electronic Materials Letters, 2012, 8, 135-139.	1.0	5
53	Plasma-Assisted Molecular Beam Epitaxy of InXGa1-XN Films on C-plane Sapphire Substrates. Korean Journal of Materials Research, 2012, 22, 185-189.	0.1	0
54	Growth Characteristics of AlN by Plasma-Assisted Molecular Beam Epitaxy with Different Al Flux. Korean Journal of Materials Research, 2012, 22, 539-544.	0.1	0

#	Article	IF	CITATIONS
55	A simple fabrication method of randomly oriented polycrystalline zinc oxide nanowires and their application to gas sensing. Advances in Natural Sciences: Nanoscience and Nanotechnology, 2011, 2, 015002.	0.7	6
56	Growth and optical properties of ZnO nanorods prepared through hydrothermal growth followed by chemical vapor deposition. Journal of Alloys and Compounds, 2011, 509, 5137-5141.	2.8	32
57	Polyaniline–chitosan nanocomposite: High performance hydrogen sensor from new principle. Sensors and Actuators B: Chemical, 2011, 160, 1020-1025.	4.0	40
58	Raman and emission characteristics of a-plane InGaN/GaN blue-green light emitting diodes on r-sapphire substrates. Journal of Applied Physics, 2011, 109, 043103-043103-4.	1.1	10
59	Suppression of composition modulation in Inâ€rich In <sub><i>x</i></sub> Ga <sub>1â^'<i>x</i></sub> N layer with high In content ( <i>x</i> â^¼â€‰0.67). Physica Status Solidi (A) Applications and Materials Scien 2011, 208, 2737-2740.	c@.8	0
60	Enhanced Photoelectrochemical Activity of the TiO <sub>2</sub> /ITO Nanocomposites Grown onto Singleâ€Walled Carbon Nanotubes at a Low Temperature by Nanocluster Deposition. Advanced Materials, 2011, 23, 5557-5562.	11.1	33
61	The thermal treatment effects of CrN buffer layer on crystal quality of Zn-polar ZnO films. Thin Solid Films, 2011, 519, 3417-3420.	0.8	2
62	Properties of (11–20) a-plane ZnO films on sapphire substrates grown at different temperatures by plasma-assisted molecular beam epitaxy. Thin Solid Films, 2011, 519, 6394-6398.	0.8	15
63	Effects of gallium doping on properties of a-plane ZnO films on r-plane sapphire substrates by plasma-assisted molecular beam epitaxy. Journal of Vacuum Science and Technology A: Vacuum, Surfaces and Films, 2011, 29, 03A111.	0.9	3
64	Structural Characterization of Bismuth Zinc Oxide Thin Films Grown by Plasma-Assisted Molecular Beam Epitaxy. Korean Journal of Materials Research, 2011, 21, 563-567.	0.1	0
65	Growth of Epitaxial AlN Thin Films on Sapphire Substrates by Plasma-Assisted Molecular Beam Epitaxy. Korean Journal of Materials Research, 2011, 21, 634-638.	0.1	2
66	Growth and optical properties of ZnO nanorods prepared through hydrothermal growth followed by chemical vapor deposition. , 2010, , .		2
67	Effects of strainâ€control layers on piezoelectric field and indium incorporation in InGaN/GaN blue quantum wells. Physica Status Solidi - Rapid Research Letters, 2010, 4, 221-223.	1.2	6
68	Interface and defect structures in ZnO films on m-plane sapphire substrates. Journal of Crystal Growth, 2010, 312, 238-244.	0.7	30
69	Growth of epitaxial ZnO films on Si (1 1 1) substrates with Cr compound buffer layer by plasma-assisted molecular beam epitaxy. Journal of Crystal Growth, 2010, 312, 2190-2195.	0.7	3
70	Investigation of nonpolar (112Â⁻0) a-plane ZnO films grown under various Zn/O ratios by plasma-assisted molecular beam epitaxy. Journal of Crystal Growth, 2010, 312, 2196-2200.	0.7	23
71	Investigation of initial growth and very thin () ZnO films by cross-sectional and plan-view transmission electron microscopy. Applied Surface Science, 2010, 256, 1849-1854.	3.1	9
72	Microstructural investigation of ZnO films grown on (111) Si substrates by plasma-assisted molecular beam epitaxy. Journal of Crystal Growth, 2010, 312, 1557-1562.	0.7	5

#	Article	IF	CITATIONS
73	Effects of low temperature ZnO and MgO buffer thicknesses on properties of ZnO films grown on (0001) Al2O3 substrates by plasma-assisted molecular beam epitaxy. Thin Solid Films, 2010, 519, 223-227.	0.8	12
74	Synthesis of porous CuO nanowires and its application to hydrogen detection. Sensors and Actuators B: Chemical, 2010, 146, 266-272.	4.0	142
75	Nanocomposite of cobalt oxide nanocrystals and single-walled carbon nanotubes for a gas sensor application. Sensors and Actuators B: Chemical, 2010, 150, 160-166.	4.0	68
76	Enhancement of CO gas sensing properties in ZnO thin films deposited on self-assembled Au nanodots. Sensors and Actuators B: Chemical, 2010, 151, 127-132.	4.0	53
77	Anisotropic properties of periodically polarity-inverted zinc oxide structures. Journal of Applied Physics, 2010, 107, 123519.	1.1	2
78	Investigations on growth and hydrogen gas sensing property of ZnO nanowires prepared by hydrothermal growth. , 2010, , .		0
79	High-Quality p-Type ZnO Films Grown by Co-Doping of N and Te on Zn-Face ZnO Substrates. Applied Physics Express, 2010, 3, 031103.	1.1	30
80	Growth of self-standing GaN substrates. , 2010, , .		0
81	Effects of Basal Stacking Faults on Electrical Anisotropy of Nonpolar a-Plane (\$11ar{2}0\$) GaN Light-Emitting Diodes on Sapphire Substrate. IEEE Photonics Technology Letters, 2010, 22, 595-597.	1.3	29
82	NO gas sensing properties of ZnO wire-like thin films synthesized by thermal oxidation of sputtered Zn metallic films in air. , 2010, , .		0
83	Origin of second-order nonlinear optical response of polarity-controlled ZnO films. Applied Physics Letters, 2009, 94, .	1.5	16
84	Structural and optical investigations of periodically polarity inverted ZnO heterostructures on (0001) Al2O3. Applied Physics Letters, 2009, 94, 141904.	1.5	10
85	Synthesis and hydrogen gas sensing properties of ZnO wirelike thin films. Journal of Vacuum Science and Technology A: Vacuum, Surfaces and Films, 2009, 27, 1347-1351.	0.9	31
86	Spontaneous transition in preferred orientation of GaN domains grown on r-plane sapphire substrate from [112Â⁻0] to [0001]. Applied Physics Letters, 2009, 94, 102103.	1.5	5
87	ZnO nanowires prepared by hydrothermal growth followed by chemical vapor deposition for gas sensors. Journal of Vacuum Science & Technology B, 2009, 27, 1667-1672.	1.3	20
88	Effects of two-step growth by employing Zn-rich and O-rich growth conditions on properties of (1120) ZnO films grown by plasma-assisted molecular beam epitaxy on sapphire. Journal of Vacuum Science & Technology B, 2009, 27, 1635.	1.3	6
89	Lateral arrays of vertical ZnO nanowalls on a periodically polarity-inverted ZnO template. Nanotechnology, 2009, 20, 235304.	1.3	6
90	Dynamic Characteristics of Metal-Induced Laterally Crystallized Polycrystalline Silicon Thin-Film Transistor Devices and Circuits Fabricated with Asymmetric Precrystallization. Japanese Journal of Applied Physics, 2009, 48, 020205.	0.8	2

#	Article	IF	CITATIONS
91	Growth and structural properties of ZnO films on (10â^'10) m-plane sapphire substrates by plasma-assisted molecular beam epitaxy. Journal of Vacuum Science & Technology B, 2009, 27, 1625.	1.3	21
92	Ultrastructural observation of electron irradiation damage of lamellar bone. Journal of Materials Science: Materials in Medicine, 2009, 20, 959-965.	1.7	10
93	Nanostructural analysis of trabecular bone. Journal of Materials Science: Materials in Medicine, 2009, 20, 1419-1426.	1.7	23
94	Electrical and magnetic properties of Mn-doped Si thin films. Physica B: Condensed Matter, 2009, 404, 1686-1688.	1.3	6
95	Hydride vapor phase epitaxy of GaN on the vicinal c-sapphire with a CrN interlayer. Journal of Crystal Growth, 2009, 311, 470-473.	0.7	5
96	Microstructural Analysis of Void Formation Due to a NH4Cl Layer for Self-Separation of GaN Thick Films. Crystal Growth and Design, 2009, 9, 2877-2880.	1.4	5
97	Structural and stimulated emission characteristics of diameter-controlled ZnO nanowires using buffer structure. Journal Physics D: Applied Physics, 2009, 42, 225403.	1.3	5
98	Effect of Refined Nitridation of Sapphire Substrates in Hydride Vapor Phase Epitaxy: Definite Correlation of Structural Characteristics between a Low-Temperature-Grown Buffer Layer and a Subsequent High-Temperature-Grown Layer of GaN. Journal of the Korean Physical Society, 2009, 54, 2404-2408.	0.3	0
99	Growth of Polarity-Controlled ZnO Films on (0001) Al2O3. Journal of Electronic Materials, 2008, 37, 736-742.	1.0	14
100	Strong enhancement of emissions from nanostructured ZnO thin films grown by plasmaâ€assisted molecularâ€beam epitaxy on nanopored Si(001) substrates. Physica Status Solidi (A) Applications and Materials Science, 2008, 205, 1598-1601.	0.8	0
101	The roles of low-temperature buffer layer for thick GaN growth on sapphire. Journal of Crystal Growth, 2008, 310, 920-923.	0.7	7
102	Effects of Zn pre-exposure temperature on the microstructures of ZnO films grown on Si(001) substrates by plasma-assisted molecular beam epitaxy. Journal of Crystal Growth, 2008, 310, 1118-1123.	0.7	6
103	Characterization of microstructure and defects in epitaxial ZnO films on Al2O3 substrates by transmission electron microscopy. Journal of Crystal Growth, 2008, 310, 4102-4109.	0.7	26
104	Reduction of dislocations in GaN films on AlN/sapphire templates using CrN nanoislands. Applied Physics Letters, 2008, 92, .	1.5	22
105	Anisotropic optical properties of free and bound excitons in highly strained A-plane ZnO investigated with polarized photoreflectance and photoluminescence spectroscopy. Applied Physics Letters, 2008, 92, 201907.	1.5	32
106	Growth and structural properties of m-plane ZnO on MgO (001) by molecular beam epitaxy. Applied Physics Letters, 2008, 92, 233505.	1.5	51
107	Dynamic Characteristics of Multi-Channel Metal-Induced Unilaterally Precrystallized Polycrystalline Silicon Thin-FilmTransistor Devices and Circuits. Korean Journal of Materials Research, 2008, 18, 507~510-507~510.	0.1	2
108	Plasma-Assisted Molecular-Beam Epitaxy of ZnO Films on (0001) Al2O3: Effects of the MgO Buffer Layer Thickness. Journal of the Korean Physical Society, 2008, 53, 271-275.	0.3	1

#	Article	IF	CITATIONS
109	Growth and Characterization of Zinc-Oxide Films Grown by Using Plasma-Assisted Molecular Beam Epitaxy on (111) Silicon Substrates with Ti and Titanium Compound Buffer Layers. Journal of the Korean Physical Society, 2008, 53, 276-281.	0.3	8
110	Temperature and Polarization Dependence of the Near-Band-Edge Photoluminescence in a Non-Polar ZnO Film Grownby Using Molecular Beam Epitaxy. Journal of the Korean Physical Society, 2008, 53, 288-291.	0.3	3
111	Growth and Characterization of Zinc Oxide Nanostructures on (111) Silicon Substrates with Aluminum Compound Layer. Journal of the Korean Physical Society, 2008, 53, 292-298.	0.3	10
112	Self-separated freestanding GaN using a NH4Cl interlayer. Applied Physics Letters, 2007, 91, 192108.	1.5	21
113	Polarity control of ZnO films on (0001) Al2O3 by Cr-compound intermediate layers. Applied Physics Letters, 2007, 90, 201907.	1.5	45
114	Structural investigation of nitrided c-sapphire substrate by grazing incidence x-ray diffraction and transmission electron microscopy. Applied Physics Letters, 2007, 91, 202116.	1.5	7
115	Structural and optical properties of non-polar A-plane ZnO films grown on R-plane sapphire substrates by plasma-assisted molecular-beam epitaxy. Journal of Crystal Growth, 2007, 309, 121-127.	0.7	90
116	Origin of forward leakage current in GaN-based light-emitting devices. Applied Physics Letters, 2006, 89, 132117.	1.5	148
117	Slowdown in development of self-assembled InAsâ^•GaAs(001) dots near the critical thickness. Journal of Vacuum Science & Technology B, 2006, 24, 1886.	1.3	3
118	Control of the ZnO Nanowires Nucleation Site Using Microfluidic Channels. Journal of Physical Chemistry B, 2006, 110, 3856-3859.	1.2	41
119	Magnetic and electrical properties of MBE-grown (Ge1â^'xSix)1â^'yMny thin films. Current Applied Physics, 2006, 6, 478-481.	1.1	11
120	Magneto-transport properties of amorphous Ge1â^'xMnx thin films. Current Applied Physics, 2006, 6, 545-548.	1.1	13
121	Growth and magnetism in amorphous Si1â^xxMnx thin films grown by thermal deposition. Journal of Magnetism and Magnetic Materials, 2006, 304, e167-e169.	1.0	5
122	Observation of ferromagnetism and anomalous Hall effect in laser-deposited chromium-doped indium tin oxide films. Solid State Communications, 2006, 137, 41-43.	0.9	44
123	Control of crystal polarity in oxide and nitride semiconductors by interface engineering. Journal of Electroceramics, 2006, 17, 255-261.	0.8	8
124	The Growth of ZnO on CrN Buffer Layer Using Surface Phase Control by Plasma Assisted Molecular-beam Epitaxy. Materials Research Society Symposia Proceedings, 2006, 957, 1.	0.1	0
125	Structural and Optical Properties of ZnO Thin Films Grown on SiO2/Si(100) Substrates by RF Magnetron Sputtering. Korean Journal of Materials Research, 2006, 16, 360-366.	0.1	1
126	Nanostructure formation and emission characterization of blue emission InN/GaN quantum well with thin InN well layers. Journal of Crystal Growth, 2005, 281, 349-354.	0.7	14

#	Article	IF	CITATIONS
127	Ferromagnetism and anomalous Hall effect in Mn-doped ZnO thin films grown by reactive sputtering. , 2005, , .		0
128	ZnO epitaxial layers grown on c-sapphire substrate with MgO buffer by plasma-assisted molecular beam epitaxy (P-MBE). Semiconductor Science and Technology, 2005, 20, S13-S21.	1.0	62
129	Ferromagnetism and Anomalous Hall Effect in p-Zn0.99Mn0.01O:P. Journal of Magnetics, 2005, 10, 95-98.	0.2	6
130	Influence of growth flux and surface supersaturation on InGaAs/GaAs strain relaxation. Applied Physics Letters, 2004, 84, 1085-1087.	1.5	5
131	Doping effects in ZnO layers using Li3N as a doping source. Journal of Crystal Growth, 2003, 251, 628-632.	0.7	9
132	Study on MgO buffer in ZnO layers grown by plasma-assisted molecular beam epitaxy on Al2O3(0001). Thin Solid Films, 2003, 445, 213-218.	0.8	24
133	Nanoheteroepitaxy of GaN on a nanopore array Si surface. Applied Physics Letters, 2003, 83, 1752-1754.	1.5	65
134	Correlation of surface chemistry of GaAs substrates with growth mode and stacking fault density in ZnSe epilayers. Journal of Vacuum Science and Technology A: Vacuum, Surfaces and Films, 2002, 20, 1948.	0.9	2
135	Control of ZnO film polarity. Journal of Vacuum Science & Technology an Official Journal of the American Vacuum Society B, Microelectronics Processing and Phenomena, 2002, 20, 1656.	1.6	17
136	Control of crystal polarity in a wurtzite crystal: ZnO films grown by plasma-assisted molecular-beam epitaxy on GaN. Physical Review B, 2002, 65, .	1.1	100
137	Morphology evolution of ZnO(000 1̄) surface during plasma-assisted molecular-beam epitaxy. Applied Physics Letters, 2002, 80, 1358-1360.	1.5	57
138	Investigation of ZnO epilayers grown under various Zn/O ratios by plasma-assisted molecular-beam epitaxy. Journal of Applied Physics, 2002, 92, 4354-4360.	1.1	122
139	Interface Engineering in ZnO Epitaxy. Physica Status Solidi (B): Basic Research, 2002, 229, 803-813.	0.7	10
140	Control of polarity of heteroepitaxial ZnO films by interface engineering. Applied Surface Science, 2002, 190, 491-497.	3.1	21
141	A challenge in molecular beam epitaxy of ZnO: control of material properties by interface engineering. Thin Solid Films, 2002, 409, 153-160.	0.8	36
142	Improvement in crystallinity of ZnSe by inserting a low-temperature buffer layer between the ZnSe epilayer and the GaAs substrate. Journal of Crystal Growth, 2002, 242, 95-103.	0.7	20
143	Effects of an extremely thin buffer on heteroepitaxy with large lattice mismatch. Applied Physics Letters, 2001, 78, 3352-3354.	1.5	89
144	Band alignment at a ZnO/GaN (0001) heterointerface. Applied Physics Letters, 2001, 78, 3349-3351.	1.5	125

#	Article	IF	CITATIONS
145	Low stacking-fault density in ZnSe epilayers directly grown on epi-ready GaAs substrates without GaAs buffer layers. Applied Physics Letters, 2001, 78, 165-167.	1.5	55
146	ZnO and related materials: Plasma-Assisted molecular beam epitaxial growth, characterization and application. Journal of Electronic Materials, 2001, 30, 647-658.	1.0	31
147	ZnO epilayers on GaN templates: Polarity control and valence-band offset. Journal of Vacuum Science & Technology an Official Journal of the American Vacuum Society B, Microelectronics Processing and Phenomena, 2001, 19, 1429.	1.6	28
148	Structural characteristics and magnetic properties of λ-MnO2 films grown by plasma-assisted molecular beam epitaxy. Journal of Applied Physics, 2001, 90, 351-354.	1.1	23
149	Stimulated emission and optical gain in ZnO epilayers grown by plasma-assisted molecular-beam epitaxy with buffers. Applied Physics Letters, 2001, 78, 1469-1471.	1.5	173
150	Evolution of initial layers of plasma-assisted MBE grown ZnO on (0001)GaN/sapphire. Journal of Crystal Growth, 2000, 214-215, 81-86.	0.7	30
151	Two-dimensional growth of ZnO films on sapphire(0001) with buffer layers. Journal of Crystal Growth, 2000, 214-215, 87-91.	0.7	42
152	Defect characterization in epitaxial ZnO/epi-GaN/Al2O3 heterostructures: transmission electron microscopy and triple-axis X-ray diffractometry. Journal of Crystal Growth, 2000, 209, 537-541.	0.7	47
153	Formation and properties of self-organized Il–VI quantum islands. Thin Solid Films, 2000, 367, 68-74.	0.8	55
154	Characterization of ZnSe/ZnMgBeSe single quantum wells. Physica E: Low-Dimensional Systems and Nanostructures, 2000, 7, 576-580.	1.3	3
155	Control and characterization of ZnO/GaN heterointerfaces in plasma-assisted MBE-grown ZnO films on GaN/Al2O3. Applied Surface Science, 2000, 159-160, 441-448.	3.1	30
156	Plasma-assisted molecular beam epitaxy for ZnO based II–VI semiconductor oxides and their heterostructures. Journal of Vacuum Science & Technology an Official Journal of the American Vacuum Society B, Microelectronics Processing and Phenomena, 2000, 18, 1514.	1.6	34
157	Control of polarity of ZnO films grown by plasma-assisted molecular-beam epitaxy: Zn- and O-polar ZnO films on Ga-polar GaN templates. Applied Physics Letters, 2000, 77, 3571-3573.	1.5	63
158	Plasma-assisted molecular-beam epitaxy of ZnO epilayers on atomically flat MgAl2O4(111) substrates. Applied Physics Letters, 2000, 76, 245-247.	1.5	98
159	Origin of hexagonal-shaped etch pits formed in (0001) GaN films. Applied Physics Letters, 2000, 77, 82-84.	1.5	99
160	Layer-by-layer growth of ZnO epilayer on Al2O3(0001) by using a MgO buffer layer. Applied Physics Letters, 2000, 76, 559-561.	1.5	256
161	Ga-doped ZnO films grown on GaN templates by plasma-assisted molecular-beam epitaxy. Applied Physics Letters, 2000, 77, 3761-3763.	1.5	361
162	Non-alloyed Au/p-ZnSe/p-BeTe ohmic contact layers for ZnSe-based blue-green laser diodes. Electronics Letters, 1999, 35, 1740.	0.5	3

#	Article	IF	CITATIONS
163	Evaluation of nanopipes in MOCVD grown (0001) GaN/Al2O3 by wet chemical etching. Journal of Crystal Growth, 1998, 191, 275-278.	0.7	57
164	Determination of defect types of ZnSe-based epilayers by etch-pit configurations. Journal of Crystal Growth, 1997, 181, 343-350.	0.7	3
165	Influence of sputtering pressure on the microstructure evolution of AlN thin films prepared by reactive sputtering. Thin Solid Films, 1995, 261, 148-153.	0.8	52
166	Microstructural degradation during Zn diffusion in a GalnAsP/InP heterostructure: Layer mixing, misfit dislocation generation, and Zn3P2precipitation. Journal of Applied Physics, 1992, 72, 4063-4072.	1.1	14